Program Digest, 2019 IEEE International Ultrasonics Symposium (IUS)
Glasgow, Scotland, October 6-9, 2019

A High-Resolution USCT Echo Imaging Method with Reduced Data-Acquisition

1st Tianhan Tang
Department of Bioengineering
The University of Tokyo
Tokyo, Japan
tang@bmpe.t.u-tokyo.ac.jp

2nd Takashi Azuma
Department of Bioengineering
The University of Tokyo
Tokyo, Japan
azuma@fel.t.u-tokyo.ac.jp

3rd Ichiro Sakuma
Department of Bioengineering
The University of Tokyo
Tokyo, Japan
sakuma@bmpe.t.u-tokyo.ac.jp

***Abstract*—In recent years, ultrasound computed tomography (USCT) has been developing as an alternative to mammography for the screening/diagnosis of breast cancer because it is non-ionizing and able to create 3D volume images. The state-of-the-art USCT echo imaging method that achieves the highest possible spatial resolution is synthetic aperture (SA). However, in order to reconstruct a high-resolution image, SA requires a large number of transmissions (TX), which leads to time-consuming data-acquisition process and heavy data-storage demands, thus rendering USCT inefficient for large-scale fast screening. Here, we propose a new imaging method that enables using 1/10 less TX to reconstruct images with even better spatial resolution than SA. Instead of using back-projection which is the basis of SA, we formulate the USCT imaging problem into a large linear equation system and reconstruct the image by solving the inversion problem. This new method is valuable in promoting the application of USCT in the large-scale fast screening of breast cancer, since reducing of TX leads to faster data-acquisition and less data-storage demands.**

***Index Terms*—USCT, ultrasound, synthetic aperture, inverse problem, simulation**

I. Introduction

Breast cancer is a significant threat to women. According to the World Health Organization (WHO)'s Global Cancer Observatory, breast cancer is the most common cancer among women world-widely, accounting for 24.2% of all cancer incidence among women (based on GLOBOCAN 2018 data) [1].

In recent years, ultrasound computed tomography (USCT) has gained increasing research focus as an alternative to mammography for the diagnosis of breast cancer [2], [3]. USCT is non-ionizing, not hampered by dense breast. It has superior spatial resolution than conventional ultrasound, and provide not only the anatomic geometry information (via the conventional B-mode image) but also quantitative information (via sound speed map and attenuation map) [2]. The current gold standard screen tool for breast cancer is X-ray based mammography. However, the disadvantages of mammography are that, first, it exposes patients to X-ray radiation; second, if the mammary glands ratio is high, the successful detection rate is low [4].

However, the problem of USCT is that it needs a large number of data acquisitions for high spatial resolution image reconstruction, which leads to a massive amount of raw data that imposes heavy demands on data storage. Also, the process itself is relatively time-consuming (compared with the conventional US) which impedes the temporal resolution of USCT. The modern USCT system usually consists of thousands of elements arranged on a ring, covering the full 360 degrees of view with a small angular step. Although there is a large degree of freedom in data acquisition strategies, a common method for echo-mode imaging is synthetic aperture (SA) [5], [6]. Consider a prototype system with 2048 elements configured on a ϕ-230 mm ring, assuming the sound speed is 1540 m/s and the sampling frequency is 20 MHz, if we use 256 times of transmission (TX) with successive 256-element apertures and all elements for receiving the signal per TX, the data acquisition process will consume about 76.5 ms, and the resulted raw data set will have size on the order of 10 GB (single-precision floating-point data type is assumed). Although it is not unmanageable to cope with data set of such size given the current technology, it is definitely not an efficient approach to adopt, especially when noting that the size of a 2D USCT image reconstructed from the raw data set is merely on the order of several MB (8-bit depth, 512-by-512 pixels assumed). Also, thinking that the surgeon will need a 3D image which consists of tens of 2D slices for the whole breast evaluation, the problem of high demands on storage and relatively low imaging speed will be magnified and may render the diagnosis process even more inefficient and prohibit the use of USCT for fast screening on large population.

In order to promote the application of USCT in breast concert diagnosis and fast screening, we propose a new USCT imaging method that uses reduced data acquisitions, while at the same time maintain high spatial resolution. Although most of the researches on USCT focus on transmissive mode (especially sound speed mode) of USCT to pursue quantitative and functional imaging, we focus on echo mode imaging in this research since it is the pillar of US/USCT and it provides the anatomical information that is primary for diagnostic evaluation.

This new method is valuable in promoting the application of USCT in the large-scale fast screening of breast cancer since reduced data acquisition via reduced TX number leads to faster data-acquisition and less data-storage demands.

II. Method

A. A Geometric View of USCT Echo Imaging

We start investigating the intrinsic properties of USCT echo imaging by considering the simplest case, i.e., a single point scatterer within the ROI of a system with infinite elements (as shown in Fig. 1a). Assume the USCT system has radius R, for an arbitrary point scatterer located inside the ROI, denote its location by (d, β) in a polar coordinate system whose origin is at the center of the ring. Using the same convention, denote the position of an arbitrary TX element (a point on the ring of infinite elements) and an arbitrary RX element by (R, α) and (R, β), respectively. With the help of *law of cosine*, one can calculate the travel distance for TX (from the TX element to the point scatterer) and RX (from the point scatterer to the RX element) by,

$$d_{TX} = \sqrt{R^2 + r^2 - 2R \cdot r \cdot \cos(\alpha - \theta)} \tag{1a}$$

$$d_{RX} = \sqrt{R^2 + r^2 - 2R \cdot r \cdot \cos(\beta - \theta)} \tag{1b}$$

When one element is used for TX (denoted as a green point on the ring in Fig. 1a), and all other elements are used for RX, the received signal contains information about the two-way travel time (i.e., t_{TX+RX}) from the TX element to the point scatterer and back to all the RX elements. If sound speed can be assumed constant during this process, the two-way travel time is proportional to the two-way travel distance (i.e., $t_{TX+RX} \propto D = d_{TX} + d_{RX}$, and $t_{TX+RX} = D/c$, where c is sound speed). Under ideal conditions, i.e., TX with delta pulse, no attenuation, and infinite sampling frequency, one can plot the trace of two-way travel distance against each corresponding RX element (as shown in Fig. 1b). Since the position of each RX element on the ring can be uniquely identified by β (where $\beta \in [-\pi, \pi)$), the plot in Fig. 1b is referred as "β-D" trace in the following part of this paper. Upon investigating a point scatterer with a given TX event, (R, α) is known system parameter, (r, θ) is constant (although unknown). Therefore, the "β-D" trace can be explicitly formulated as a continuous function,

$$\begin{aligned} D(\beta) := &\sqrt{R^2 + r^2 - 2R \cdot r \cdot \cos(\alpha - \theta)} \\ &+ \sqrt{R^2 + r^2 - 2R \cdot r \cdot \cos(\beta - \theta)} \end{aligned} \tag{2}$$

One can observe that the position information of the point scatterer (r, θ) is embedded in the "β-D" trace (while the echogenicity information is embedded in the amplitude of the received signal). Moreover, it can be shown that for a fixed TX event (i.e., fixed (R, α)), for a specific point scatterer, the "β-D" is different from that of any other point scatterer. By linear acoustics theory, when multiple point scatterers present in the ROI, the received data will be the combination of all those unique patterns resulted from every individual point scatterer. Thus, it is deduced that if one can differentiate each unique pattern from the received data, one can recover the distribution of each point scatterer. Together with the amplitude information in the received data which gives information about the echogenicity of each point scatterer, one completely resolves the echo imaging problem. It can be shown that theoretically, one can recover the position of infinite scatterer points, given an infinite number of elements on the ring, and infinite sampling frequency.

B. The Proposed USCT Echo Imaging Method

Although in practice, only finite number of elements and finite sampling frequency are available, and the object (biological tissue) under investigation is usually a continuous medium, two considerations can help successful application of the idea presented in the preceding section to USCT echo imaging. First, it is important to recall that image reconstruction is also a problem with finite variables. Ultimately, it is just a problem of assigning a finite number of pixels of an image with appropriate values. Thus it is reasonable to infer that only a finite amount of information is necessary. Second, the ROI is implicitly divided into small (pixel) grids during the image reconstruction process. As long as the grid size is sufficiently small, one can treat the cumulative signal from the continuous medium within a pixel grid as generated by a representative single point scatterer at the center of that grid. Based on those two considerations, for a given object, its echo image can be regarded as the distribution of the point scatterers with different echogenicity constituting that object in the ROI. Once again, the linear acoustics theory allows us to consider the received signal of investigating the object under a given TX-RX configuration as the linear combination of the signal coming from point scatterers in each grid. If one could know the received signal pattern from a single point scatterer at every possible grid position in advance, one can use it as a reference to decode the actual distribution of point scatterers from the received data.

The proposed method simulates the received signal with a given TX-RX configuration and a given ROI setup, assuming that there was only one point scatterer with unit echogenicity within each grid, and rearrange the simulated signal into a matrix G, called the measurement matrix. Each column of G is an unrolled 1-D vector of the received signal from every RX channels for a specific point scatterer. Denote the number of TX by nTX, number of RX by nRX, number of samples for each RX channel by nS, number of pixels in each row (assuming a square image) by nP, then G is of size $nTX \times nRX \times nS$-by-$nP \times nP$. The 2-D array of pixel values can also be unrolled into a column vector with length $nP \times nP$, and is denoted it as $\mathbf{x}$. The received signal from an actual measurement with the same configuration as that used for generating the $\mathbf{G}$ matrix is unrolled into a 1-D column vector $\mathbf{y}$, with length $nTX \times nRX \times nS$. Consequently, the problem of USCT echo imaging is formulated into a system of linear equations, represented in matrix form as,

$$\mathbf{G} \cdot \mathbf{x} = \mathbf{y} \tag{3}$$

where the *i*-th column of G is the unrolled RX signal of the point scatterer in the *i*-th corresponding pixel grid. The image

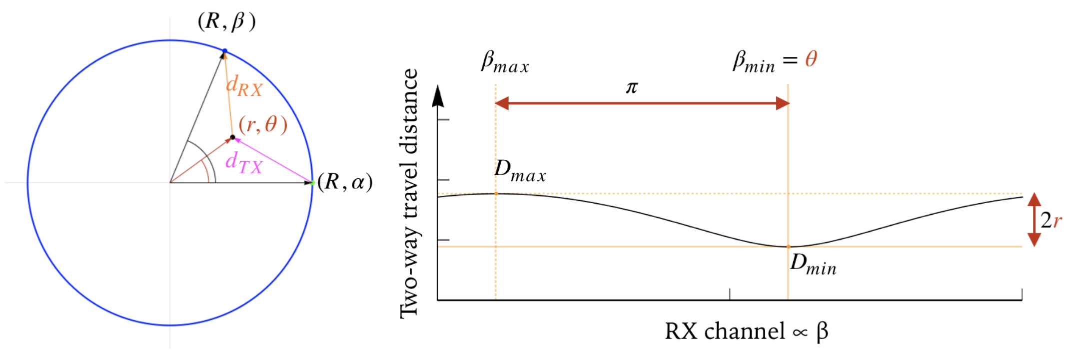

(a) (b)

Fig. 1. (a) Configuration of a single point scatterer within ROI of the USCT system with infinite number of elements (b) and the receiving channel vs. travel distance.

reconstruction is done by solving the inverse problem for $\mathbf{x}$, and partition it into an appropriate 2D format.

C. Simulation Experiment

Simulation experiments have been performed to evaluate the performance of the proposed method against the synthetic aperture method. Several assumptions are made for the simulations, i.e.,

- Homogeneous background medium is assumed, that is, we use constant sound speed for the simulation;
- Point scatterer is assumed to be small compared to the wavelength of ultrasound so that we can model the scattering process as isotropic;
- No second-order scattering is considered in the simulation by Born's approximation.

We model each transducer element as a point source and take into account the acoustic intensity loss due to the spherical spreading of energy in space. We use the power-law model to capture the attenuation of ultrasound propagating the medium and take into account the thermal noise in the practical measurement.

To suppress the effect of transmission wave (i.e., the strong passed through ultrasound signal shadows the weak scattered ultrasound signal on the opposite side of the TX element), for each TX event only several elements that centered on the one for TX are used to collect the reflected signal. A rule of thumb of about 3/8 of the total number of elements is used for RX for each TX event [6]. The numerical phantom consists of 5-by-5 point scatterers with uniform echogenicity distributed on a regular grid. The simulation conditions are summarized in Table I.

After the image reconstruction, we calculate the signal-to-noise ratio (SNR) for each point scatterer.

TABLE I
SIMULATION EXPERIMENT CONDITIONS

Parameters	Value
Number of USCT elements	2, 4, 8, 16, 32, 64, 128, 256
Number of elements for RX	1, 3, 5, 7, 11, 23, 47, 95
Diameter of USCT ring	25 mm
Sound speed	1540 m/s
Sampling frequency, f_s	16 MHz
Excitation pulse	Gaussian weighted 4-cycle sine wave
Central frequency, f_c	2 MHz
Region of interest	12.5-by-12.5 mm^2
Pixel number	50-by-50
Pixel size	0.25-by-0.25 mm^2
Medium attenuation	0.6 dB/MHz/cm/
Noise level	-60 dB

III. RESULT

Fig. 2 shows the reconstructed images under -60 dB noise level (ratio of maximum noise amplitude to signal) with a different number of elements, with SA and the proposed method, respectively.

With only 2 or 4 elements, both methods do not reveal the actual distribution of point scatterers. With 8 elements, SA gives a noisy approximation of the distribution of point scatterers. However, the proposed method still does not reveal the distribution. With more than 16 elements, the proposed method exhibits better spatial resolution than SA. Images from the proposed method with more than 128 elements are currently not available due to immense computation pressure on our current resource.

Fig. 3 compares the SNR for each image reconstructed using SA and the proposed method, respectively. The performance in terms of SNR of SA increases with the number of elements. However, it seems there is little benefit for the proposed method if a certain number is achieved. There is a quick rise of SNR for the proposed method, between 8 elements where no reasonable image is obtained, and 16 elements where near perfect recover of point scatterers distribution is obtained. With more than 16 elements, the SNR of the proposed method quickly surpasses that of SA.

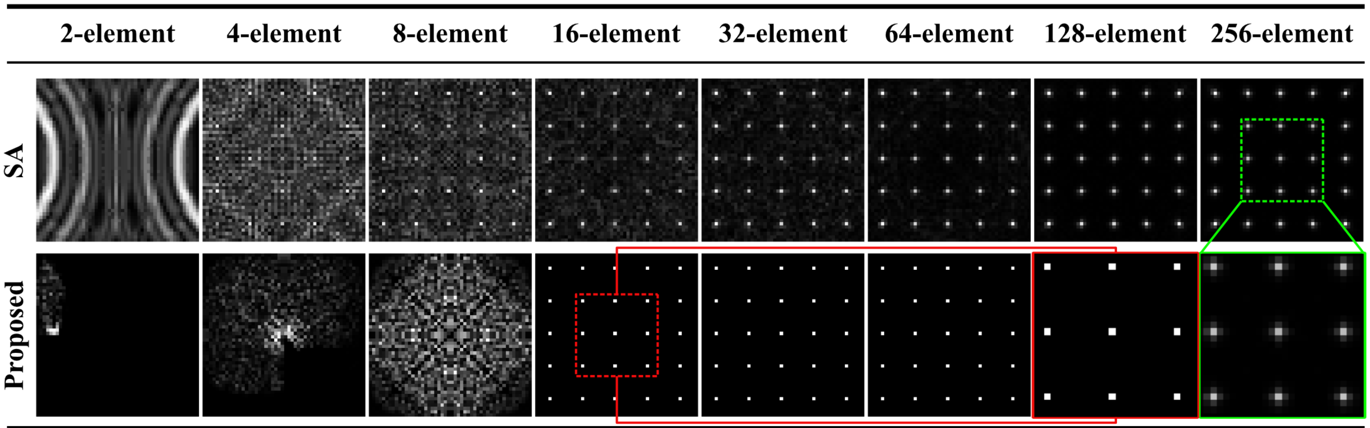

Fig. 2. Images reconstructed by SA and the proposed method with different number of USCT elements.

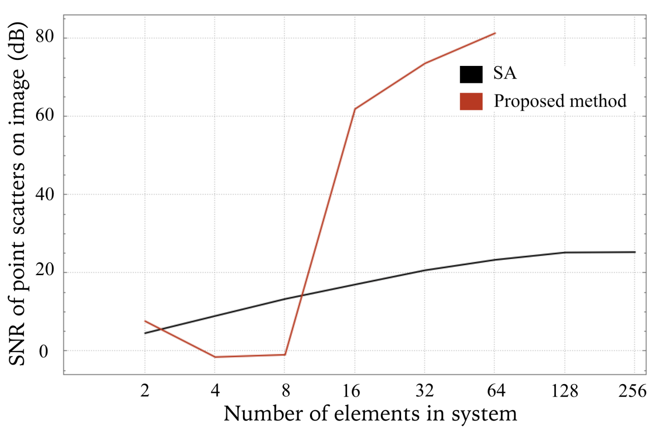

Fig. 3. Comparison of Number of elements vs. SNR for SA method and the proposed method.

IV. Discussion

The simulation experiments indicate that the proposed method is capable of both high speed (with a small number of elements) and high spatial resolution (pixel-width point spread function) imaging. When the number of elements is small, it performs superior to SA. As the number of elements increase, the performance of SA improves, while the proposed method seems not sensitive to the number of elements when certain number achieves. Future study should consider that for some specific desired criteria (e.g., resolution, SNR), how many numbers of elements is necessary. Also noting that in the current study, uniformly spaced TX/RX channel is used. Future may explore the possibility of adaptive imaging that maximizes the performance.

The most fundamental assumption of this method is linear acoustics. It currently could not handle nonlinear systems such as that includes nonuniform sound speed region. Further work should be conducted to investigate the robustness of the proposed method with experiment data.

The time cost for solving the inverse problem is high. Although the theoretical temporal resolution increase can be achieved by reducing the number of elements (for TX), the current computation can only be done off-line. The sparsity of the G measurement matrix may be utilized to construct a practical algorithm for fast processing.

V. Conclusion

This research proposed a new USCT imaging method that formulates the imaging problem into a linear equation system and performs the image reconstruction by solving the inverse problem. The simulation study indicates that the proposed method has higher spatial resolution than the conventional synthetic aperture method with much less raw data acquisition. We plan to elucidate the quantitive relation between desired image resolution and the necessary amount of data and evaluate the proposed method with experimental data in the future study.

Acknowledgment

T. Tang would like to thank Lily MedTech Inc. for the support of this work.

References

[1] F. Bray, J. Ferlay, I. Soerjomataram, R. L. Siegel, L. A. Torre, and A. Jemal, "Global cancer statistics 2018: Globocan estimates of incidence and mortality worldwide for 36 cancers in 185 countries," *CA: a cancer journal for clinicians*, vol. 68, no. 6, pp. 394–424, 2018.

[2] C. Li, N. Duric, P. Littrup, and L. Huang, "In vivo breast sound-speed imaging with ultrasound tomography," *Ultrasound in medicine & biology*, vol. 35, no. 10, pp. 1615–1628, 2009.

[3] H. Gemmeke, T. Hopp, M. Zapf, C. Kaiser, and N. V. Ruiter, "3d ultrasound computer tomography: Hardware setup, reconstruction methods and first clinical results," *Nuclear Instruments and Methods in Physics Research Section A: Accelerators, Spectrometers, Detectors and Associated Equipment*, vol. 873, pp. 59–65, 2017.

[4] N. R. Council *et al.*, *Mammography and beyond: developing technologies for the early detection of breast cancer*. National Academies Press, 2001.

[5] J. A. Jensen, S. I. Nikolov, K. L. Gammelmark, and M. H. Pedersen, "Synthetic aperture ultrasound imaging," *Ultrasonics*, vol. 44, pp. e5–e15, 2006.

[6] X. Qu, T. Azuma, T. Yogi, S. Azuma, H. Takeuchi, S. Tamano, and S. Takagi, "Synthetic aperture ultrasound imaging with a ring transducer array: preliminary ex vivo results," *Journal of Medical ultrasonics*, vol. 43, no. 4, pp. 461–471, 2016.